Thermal effects on the Wigner localization and Friedel oscillations in many-electron nanowires

I. Kylänpää,[1,*] F. Cavaliere,[2,3] N. Traverso Ziani,[4] M. Sassetti,[2,3] and E. Räsänen[1]

[1]*Department of Physics, Tampere University of Technology, P.O. Box 692, FI-33101 Tampere, Finland*

[2]*Dipartimento di Fisica, Universitá degli Studi di Genova, Via Dodecaneso 33, 16146 Genova, Italy*

[3]*CNR-SPIN, Via Dodecaneso 33, 16146 Genova, Italy*

[4]*Institute for Theoretical Physics and Astrophysics, University of Würzburg, 97074 Würzburg, Germany*

(Received 22 June 2016; revised manuscript received 24 August 2016; published 13 September 2016)

Thermal effects on the total charge density are studied for a one-dimensional correlated quantum dot by means of the path integral Monte Carlo method. The competition between Friedel and Wigner oscillations at zero temperature is driven by the ratio between the interaction of electronic strength and the kinetic energy of electrons. At the onset of the formation of a Wigner molecule, we show that thermal enhancement of Wigner oscillations occurs in a range of temperatures, which can be observed in the electron density. We further show that low-temperature Friedel oscillations may change to Wigner oscillations upon an increase in the temperature.

DOI: 10.1103/PhysRevB.94.115417

I. INTRODUCTION

In finite-size one-dimensional (1D) systems such as 1D quantum dots [1,2] corresponding to nanowires with longitudinal confinement, a strong competition between finite-size effects and electronic interactions occurs. This may give rise to peculiar charge density oscillations.

Due to quantum confinement of N electrons (in a region of length l), the so-called Friedel oscillations of the electronic density typically occur [3]. In the ground state, they are characterized by a wave vector $2k_F$, where $k_F = \pi N/2l$, and in the density they give rise to $N/2$ peaks [4]. Such oscillations are induced by the backscattering of electrons near the edges of the system.

Interactions between electrons are also responsible for oscillations in the electron density. When interactions dominate over the average kinetic energy, electrons eventually arrange themselves into N positions, giving rise to oscillations with a wave vector $4k_F$ and N peaks in the total electron density. Such a correlated state is called a *Wigner molecule* [5,6] and constitutes the finite-size counterpart of a Wigner crystal [7]. The physical properties of a Wigner molecule are only quantitatively affected by different types of quantum confinement, but in the absence of spin-orbit coupling [8] or spin-momentum locking [9], N peaks in the density are always present.

A 1D dot breaks all spatial symmetries (barring parity), allowing for oscillations to appear already at the level of the total charge density. Hence, in principle, by counting the number of peaks in the density we can assess whether Friedel or Wigner physics dominates. This is in contrast to higher-dimensional systems that have specific symmetries such as two-dimensional circular quantum dots [10–15]. In such systems density-density correlation functions [3] are required to properly assess the formation of a molecular state. Notwithstanding this, it has been questioned that density oscillations alone are a valid signature of the presence of a Wigner molecule even in one dimension, and correlation functions have been proposed even in this case [16,17].

The computational complexity in the study of Wigner molecules scales exponentially with N, so that the numerically exact diagonalization [18–24] method becomes very inefficient already for $N \sim 10$ (even in one dimension). For larger N, quantum Monte Carlo methods [25] provide a powerful technique for many-body simulations. In the path integral Monte Carlo (PIMC) formulation [26–29], thermal effects can be studied by accurate quantum statistical simulations. On the other hand, in the opposite limit of a very large number of electrons, the Luttinger liquid theory [30–40] is an efficient tool to obtain analytically the density and density-density correlation functions both at zero and at finite temperatures. It allows us to conveniently evaluate transport properties, which constitute an important tool to assess the presence of Friedel and Wigner oscillations [38,40,41].

Recently, intriguing effects have been found near the crossover between Friedel and Wigner oscillations. In particular, increasing the temperature may *enhance* the localization of the electrons. Only at sufficiently high temperatures does the conventional *melting* [42,43] occur, leading to a smeared nonoscillating density. This phenomenon has been predicted in the large-N limit by means of the Luttinger liquid theory, and it is associated with the wide separation of the energy scales of spin and charge collective excitations of the system [40]. The thermal enhancement of Wigner oscillations has also been predicted for $N = 2$ by exact diagonalization calculations [24] and proven to be induced by the collapse of the triplet-singlet energy gap as the dot approaches the Friedel-Wigner transition for $T = 0$. Generally, when thermal fluctuations exceed the collective spin excitation energy or the triplet-singlet gap, enhanced Wigner oscillations are induced by thermal populations of excited states [24].

In this paper, we fill the gap in the present literature regarding the thermal properties of 1D systems near the Friedel-Wigner crossover. We employ a numerically accurate PIMC method to calculate total electron densities for 1D nanowires with $N = 2 \ldots 20$. Our results show thermal enhancement of the Wigner localization, which is pronounced in the intermediate interaction regime. Our results constitute evidence that the thermal enhancement of the Wigner localization is a ubiquitous phenomenon which shows up for an arbitrary number of electrons in the dot.

*ilkka.kylanpaa@tut.fi

II. MODEL AND METHOD

The system [see Fig. 1(a)] consists of N electrons harmonically confined in a 1D nanowire. The electron-electron interactions are described by a scaled and softened Coulomb potential. The total Hamiltonian then reads

$$H = \sum_{i=1}^{N} \left(-\frac{\hbar^2}{2m}\frac{\partial^2}{\partial x_i^2} + \frac{m\omega^2}{2}x_i^2 \right) + \sum_{i<j} \frac{c}{\sqrt{|x_i - x_j|^2 + \lambda^2}}, \tag{1}$$

where $c \geqslant 0$ is the scaling factor of the interaction, and λ is the softening parameter used to take into account the effect of the upper subbands of the wire [20]. As in Ref. [24], we adopt the length scale $l = \sqrt{2\hbar/m\omega}$. Thus, having $E_0 = \hbar\omega$, we get the dimensionless parameters as $\tilde{x} = x/l, \tilde{\lambda} = \lambda/l, \tilde{c} = c/(lE_0)$, and $\tilde{T} = Tk_B/E_0$. In the following, we use atomic units with $\hbar = m = 1$ and set $\omega = 1$, so that $E_0 = 1$.

The Feynman formulation of quantum statistical mechanics [44] provides path integrals for studying quantum many-body effects at finite temperature. We use the path integral Monte Carlo method [26–29] in order to accurately account for both finite-temperature and correlation effects. Fermi statistics is employed by the restricted path integral formalism [45], in which the density matrix is given as

$$\rho_F(R_\beta, R_\star; \beta) = \int dR_0 \rho_F(R_0, R_\star; 0) \int_{\gamma: R_0 \to R_\beta}^{\gamma \subset \Upsilon_\beta(R_\star)} dR_t e^{-\mathcal{S}[R_t]}, \tag{2}$$

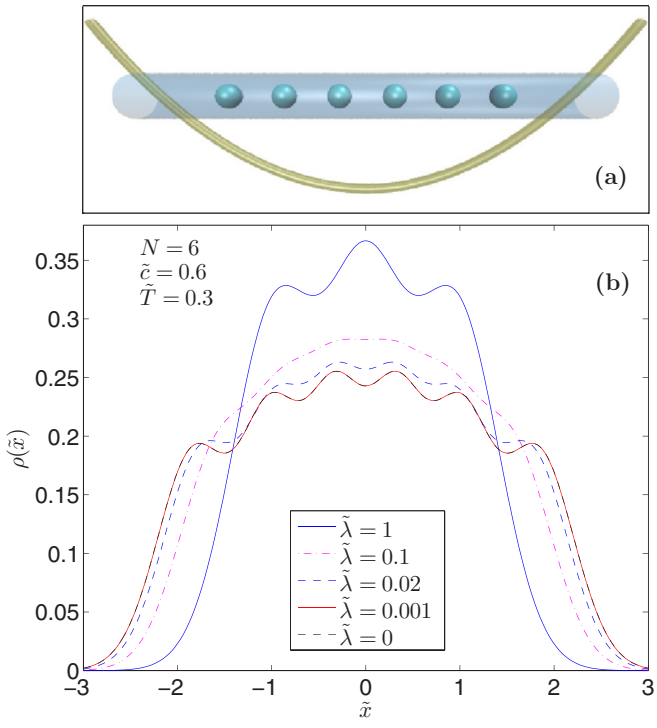

FIG. 1. (a) Schematic of the nanowire described by confined electrons in a harmonic confinement. (b) Electron density for $N = 6$ with different values of the softening parameter $\tilde{\lambda}$ in the Coulomb potential [see Eq. (1)]. The other parameters are $\tilde{c} = 0.6$ and $\tilde{T} = 0.3$.

where $\beta = 1/k_B T$, F refers to the Fermion density matrix, S is the action, $R_\star$ is the so-called reference point, and Υ_β is a region in "space-time" that specifies the boundary conditions for the Bloch equation. In this work we use the nodes of the free-particle density matrix [45] to determine the boundary conditions. We point out that for the present study the restricted path integral formalism and the free-particle nodes provide excellent accuracy due to relatively high temperatures [46]: for example, our lowest temperature $\tilde{T} = 0.1$ corresponds to 31 578 K. The sampling in the configuration space is carried out using the Metropolis procedure [47] with multilevel bisection moves [48].

Commonly, the magnetization of the system is predetermined, e.g., to be polarized or unpolarized [49,50]. However, in this case we need to include all possible spin configurations in our thermal averages [51]. This can be accomplished by including the sampling of the magnetization: we occasionally attempt to flip a spin of an electron, which is accepted or rejected depending on whether the new path configuration is legal. In this work we focus on simulations with the magnetization sampling.

III. RESULTS

A. Effects of the interaction parameters λ and *c*

In the case of two electrons our PIMC results are directly comparable to the exact-diagonalization study in Ref. [24]. The comparison (not shown here) yields no visible differences between the results. We then proceed with $N > 2$ and consider first the effect of the softening parameter $\tilde{\lambda}$ on the electron density when $N = 6$. The results for a fixed value $\tilde{c} = 0.6$ of the interaction strength and $\tilde{T} = 0.3$ for the temperature are shown in Fig. 1(b), where $\tilde{\lambda}$ describes the maximum distance between the electrons as they pass each other. Therefore, with larger values of $\tilde{\lambda}$ we find fewer peaks in the density, whereas at small values of $\tilde{\lambda}$ ($\lesssim 0.02$) we find a Wigner-crystallized state of $N = 6$ peaks. The density converges as $\tilde{\lambda} \to 0$.

From now on we use $\tilde{\lambda} > 0$, which gives the best representation for a practical 1D nanowire, where the electrons are able to pass each other. The effect of the strength parameter $\tilde{c}$ (with $\tilde{\lambda} = 0.02$) is considered next for $N = 3$ electrons. In Fig. 2 we show the electron densities of this system as a function of the temperature for interaction strengths $\tilde{c} = 0.2$, 0.4, 0.6, and 1 [Figs. 2(a)–2(d), respectively]. The sequence of Figs. 2(a)–2(d) clearly shows that, as expected, the Wigner localization increases with c. The behavior as a function of the temperature is more complex as analyzed in detail below.

B. Thermal effects on Wigner localization

The electron densities for $N = 3$ in Fig. 2 show that increasing temperature eventually leads to smearing of the density so that the localization disappears, regardless of the interaction parameter c. However, we also find *thermally enhanced localization* at low temperatures. This localization effect can be seen as an increased depth of the two valleys in the density, and it is most visible in the intermediate interaction regime with $\tilde{c} \sim 0.4$.

Thermal localization is more clearly visible in Figs. 3(a)–3(d), where we show the corresponding Fourier transforms

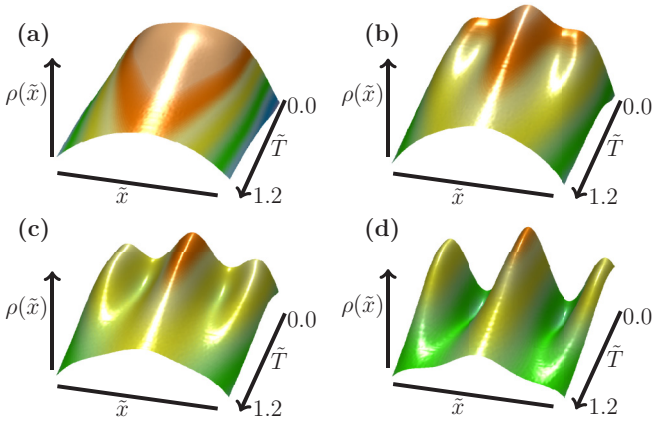

FIG. 2. Electron densities for the $N = 3$ nanowire as a function of the temperature. Four interaction strengths with $\tilde{\lambda} = 0.02$ are considered: (a) $\tilde{c} = 0.2$, (b) $\tilde{c} = 0.4$, (c) $\tilde{c} = 0.6$, and (d) $\tilde{c} = 1.0$. The temperature $\tilde{T}$ goes from 0.02 to 1.2, and $\tilde{x}$ from $-$ 1.2 to 1.2.

of the electron densities in Fig. 2. Here the wave vector k is expressed in terms of the (approximate) Fermi wave vector k_F. The main interest here is in the peaks related to $k = 2k_F$ and $k = 4k_F$, i.e., Friedel and Wigner oscillations, respectively. In Fig. 3(a) we can clearly identify only the $k = 2k_F$ peak. However, as the interaction strength parameter $\tilde{c}$ is increased through Fig. 3(b) to Fig. 3(d), the oscillations with the wave vector $4k_F$ appear with increasing amplitude. Moreover, in Figs. 3(b)–3(d) at about $k = 4k_F$ we find local maxima in $\rho(k)$ at nonzero temperatures. In other words, increasing the temperature from 0 leads to enhanced Wigner localization. However, the effect is relatively weak, and as mentioned above, it disappears as the temperature is increased further.

In Fig. 4 we consider systems with more electrons by showing the electron densities at a few temperatures: (a) $N = 4$, $\tilde{\lambda} = 0.02$, and $\tilde{c} = 0.6$; (b) $N = 6$, $\tilde{\lambda} = 0.02$, and $\tilde{c} = 0.7$; (c) $N = 10$, $\tilde{\lambda} = 0.05$, and $\tilde{c} = 0.8$. Thermal enhancement of

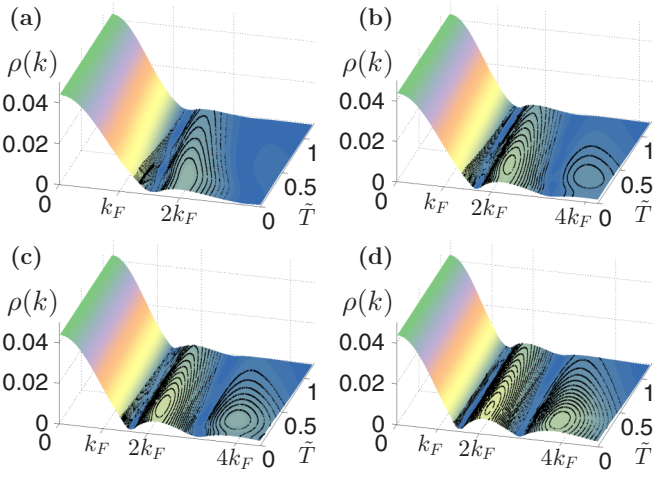

FIG. 3. Fourier transforms of the electron densities shown in Fig. 2. The second peak, at $k = 2k_F$, is characteristic of Friedel oscillations and the third peak, at $k = 4k_F$, corresponds to Wigner oscillations. The contour lines are plotted from $k = 1.3k_F$ up to larger values in steps of $\sim 3.2 \times 10^{-4}$.

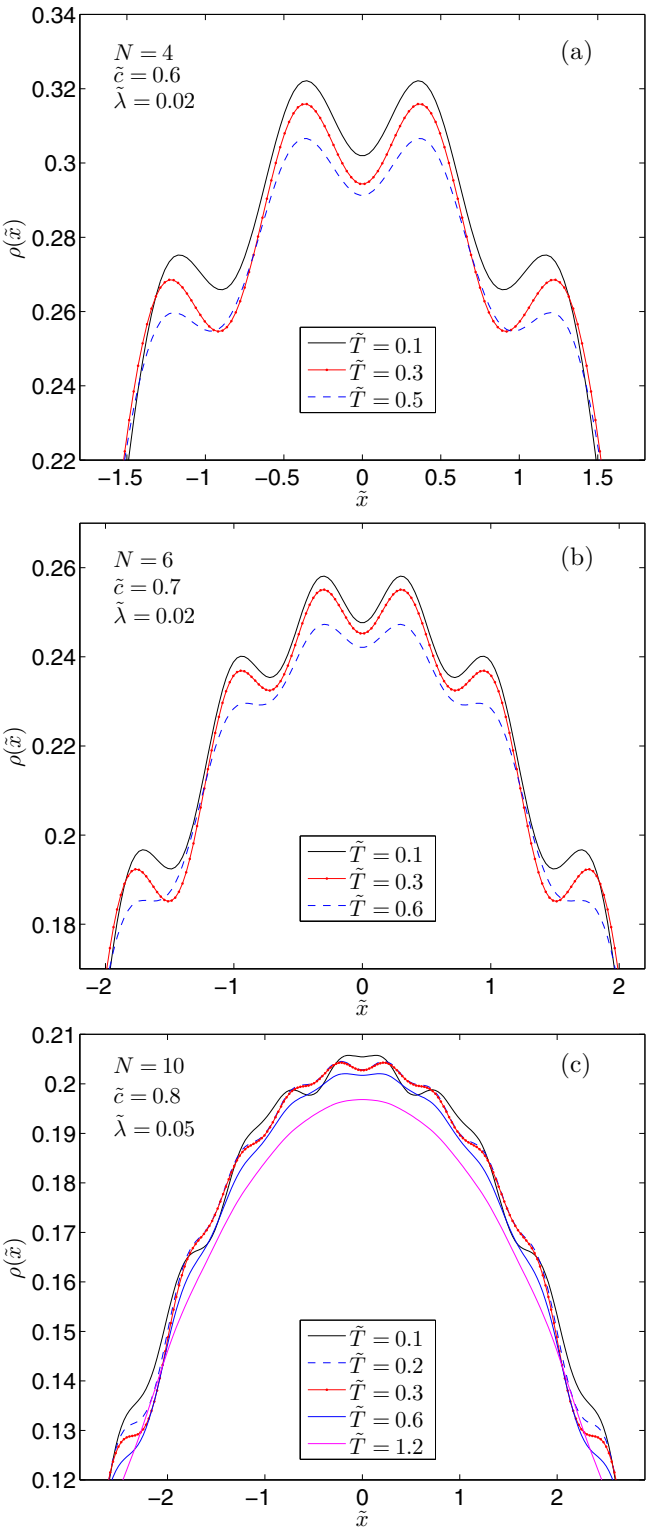

FIG. 4. Electron density of a nanowire with (a) $N = 4$, (b) $N = 6$, and (c) $N = 10$ electrons at three temperatures. Parameters $\tilde{c}$ and $\tilde{\lambda}$ are given in the figures. In all cases signatures of thermally enhanced Wigner localization are found.

the Wigner localization appears in all cases. For example, in Figs. 4(a) and 4(b) the strongest localization effect is seen for the peaks at the edges of the electron density. It should be noted that although the effect is relatively weak, it is in line with the

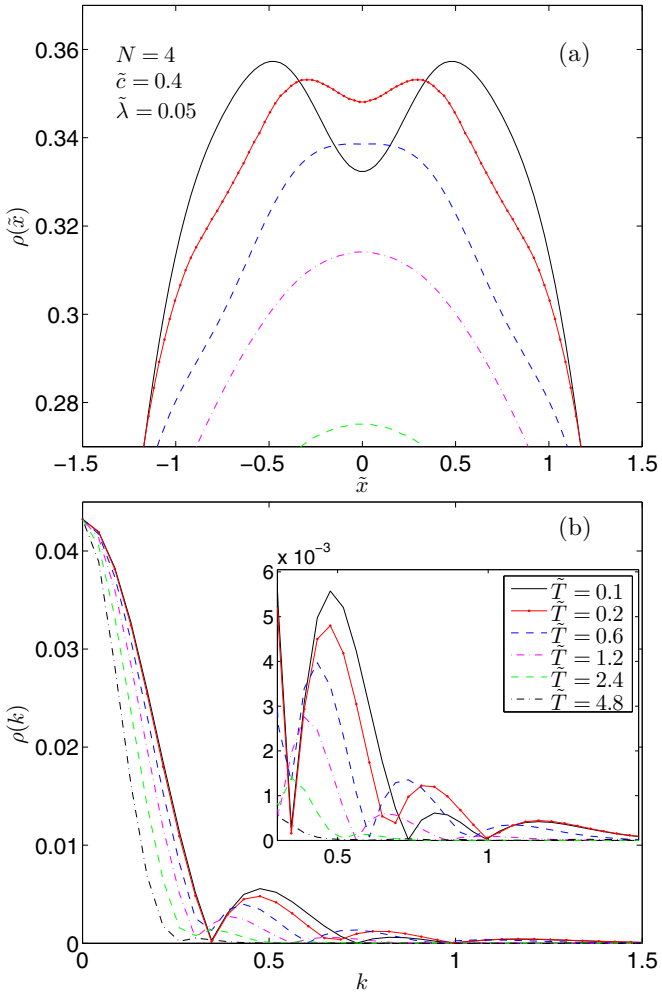

FIG. 5. (a) Electron density of a nanowire with $N = 4$, $\tilde{c} = 0.4$, and $\tilde{\lambda} = 0.05$ at temperatures given in (b), where we give the Fourier transform of the electron densities. Note that $\tilde{T} = 4.8$ is not visible for the chosen axis in (a), but its Fourier transform is in (b).

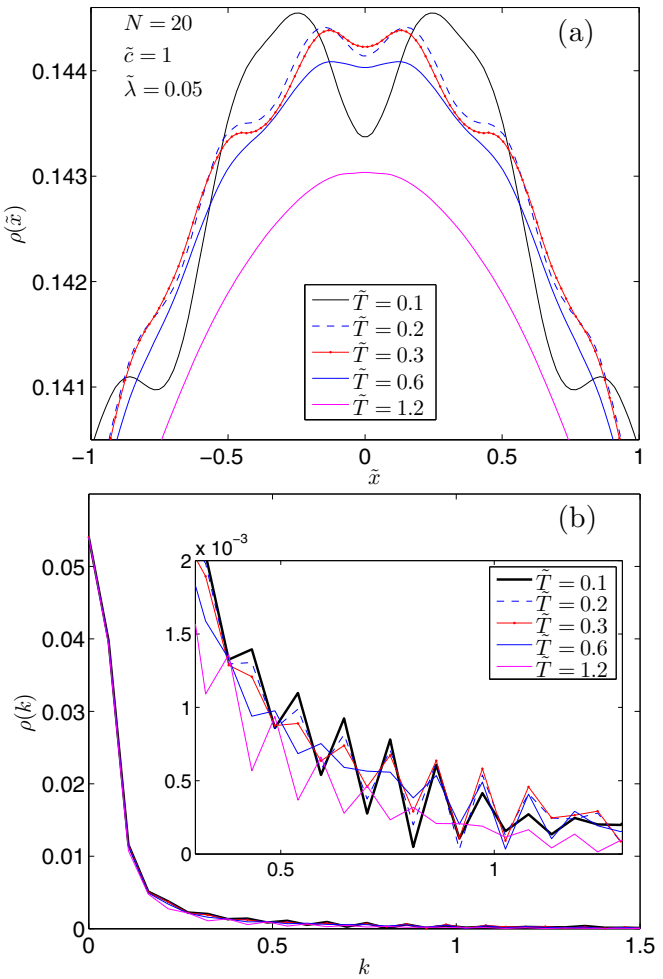

FIG. 6. (a) Electron density of a nanowire with $N = 20$, $\tilde{c} = 1.0$, and $\tilde{\lambda} = 0.05$ at temperatures given in (b), where we show the Fourier transform of the electron densities.

$N = 3$ case shown in Fig. 2, as well as with $N = 2$ considered in Ref. [24]. The results indicate that with the proper choice of the interaction parameter (and the shape of the confinement) the effect is very generic and can be found for all particle numbers.

C. Thermal transition from Friedel to Wigner oscillations

Varying the interaction strength by adjusting the parameters $\tilde{c}$ and $\tilde{\lambda}$ we can obtain Friedel oscillations at low temperatures. Depending on the balance between these parameters it is possible that the increasing temperature changes the Friedel oscillations to Wigner oscillations before the electron density eventually smears out. Within this region of the parameter space there is a coexistence of Friedel and Wigner oscillations, which can be observed in Fig. 5(a), where we show a weak transition from Friedel to Wigner in the electron density as the temperature is increased (note that we show only the top part of the density profile).

The Fourier transform of the electron density [Fig. 5(b)] shows how thermal effects may allow the $4k_F$ oscillations not only to be enhanced, but also to emerge altogether from the $2k_F$ shape. We can clearly see that at low temperatures there is a predominant peak at $2k_F$, while with an increase in the temperature the $4k_F$ component stands out more clearly. Increasing the temperature further the $4k_F$ peak seems to detune, shifting towards $k \to 0$. We see that the melting will eventually lead to a single peak in the electron density, which is relatively close to a Gaussian profile due to the harmonic confinement. Therefore, as $\tilde{T} \to \infty$ all features in the reciprocal space will coalesce into a single peak around $k = 0$.

In Fig. 6(a) we show the electron density for the largest system considered in this work, i.e., $N = 20$ with $\tilde{c} = 1.0$ and $\tilde{\lambda} = 0.05$. Again, the electron densities indicate the emergence of Wigner oscillations over Friedel oscillations as the temperature is increased—similarly to Fig. 5. In the Fourier transform in Fig. 6(b), we plot the lowest temperature result as the thick solid black line. Despite the low resolution at around $k = 1$ we can clearly see three lines that are noticeably above the low-temperature line, which indicates thermal enhancement in the oscillations.

IV. SUMMARY

To summarize, we have used the path integral Monte Carlo approach to demonstrate that thermal effects may enhance Wigner localization in one-dimensional nanowires consisting of $N \geqslant 2$ electrons that interact through the softened one-dimensional Coulomb potential. We have illustrated how the electron density is affected by the interaction parameters λ and c. Our results show that thermal enhancement of Wigner localization is found independently of the number of electrons in the quantum dot. In addition, we have identified a parameter regime where Friedel oscillations, when the temperature is increased, evolve into Wigner oscillations, which eventually smear out at even higher temperatures.

ACKNOWLEDGMENTS

We acknowledge CSC—IT Center for Science Ltd. and TCSC—Tampere Center for Scientific Computing for the allocation of computational resources. We gratefully acknowledge the support of the Academy of Finland, European Community's FP7 through the CRONOS project (Grant Agreement No. 280879) and NANOCTM (Grant Agreement No. ITN-2008-234970), MIUR via MIUR-FIRB2012—Project HybridNanoDev (Grant Agreement No. RBFR1236VV), and the Nordic Innovation through its Top-Level Research Initiative, Project no. P-13053. N.T.Z. acknowledges the financial support from the DFG (SPP1666 and SFB1170 "ToCoTronics").

[1] L. P. Kouwenhoven, D. G. Austing, and S. Tarucha, Rep. Prog. Phys. **64**, 701 (2001).
[2] J.-C. Charlier, X. Blase, and S. Roche, Rev. Mod. Phys. **79**, 677 (2007).
[3] G. F. Giuliani and G. Vignale, *Quantum Theory of the Electron Liquid* (Cambridge University Press, Cambridge, UK, 2005).
[4] For simplicity, we have assumed here that N is even, while $k_F = \pi(N+1)/2l$ if N is odd, and the Friedel oscillations display $(N+1)/2$ peaks in the density.
[5] S. M. Reimann and M. Manninen, Rev. Mod. Phys. **74**, 1283 (2002).
[6] C. Yannouleas and U. Landman, Rep. Prog. Phys. **70**, 2067 (2007).
[7] E. Wigner, Phys. Rev. **46**, 1002 (1934).
[8] F. M. Gambetta, N. T. Ziani, S. Barbarino, F. Cavaliere, and M. Sassetti, Phys. Rev. B **91**, 235421 (2015).
[9] N. T. Ziani, F. Crépin, and B. Trauzettel, Phys. Rev. Lett. **115**, 206402 (2015).
[10] M. Dineykhan and R. G. Nazmitdinov, Phys. Rev. B **55**, 13707 (1997).
[11] M. B. Tavernier, E. Anisimovas, F. M. Peeters, B. Szafran, J. Adamowski, and S. Bednarek, Phys. Rev. B **68**, 205305 (2003).
[12] M. Rontani, C. Cavazzoni, D. Bellucci, and G. Goldoni, J. Chem. Phys. **124**, 124102 (2006).
[13] A. Harju, H. Saarikoski, and E. Räsänen, Phys. Rev. Lett. **96**, 126805 (2006).
[14] A. Ghosal, A. D. Güclü, C. J. Umrigar, D. Ullmo, and H. U. Baranger, Nat. Phys. **2**, 336 (2006).
[15] U. De Giovannini, F. Cavaliere, R. Cenni, M. Sassetti, and B. Kramer, New J. Phys. **9**, 93 (2007); Phys. Rev. B **77**, 035325 (2008); F. Cavaliere, U. De Giovannini, M. Sassetti, and B. Kramer, New J. Phys. **11**, 123004 (2009).
[16] J.-J. Wang, W. Li, S. Chen, X. Gao, M. Rontani, and M. Polini, Phys. Rev. B **86**, 075110 (2012).
[17] F. M. Gambetta, N. Traverso Ziani, F. Cavaliere, and M. Sassetti, Europhys. Lett. **107**, 47010 (2014).
[18] W. Häusler and B. Kramer, Phys. Rev. B **47**, 16353 (1993).
[19] K. Jauregui, W. Häusler, and B. Kramer, Europhys. Lett. **24**, 581 (1993).
[20] A. Secchi and M. Rontani, Phys. Rev. B **80**, 041404 (2009).
[21] A. Secchi and M. Rontani, Phys. Rev. B **82**, 035417 (2010).
[22] A. Secchi and M. Rontani, Phys. Rev. B **85**, 121410 (2012).
[23] A. Secchi and M. Rontani, Phys. Rev. B **88**, 125403 (2013).
[24] F. Cavaliere, N. Traverso Ziani, F. Negro, and M. Sassetti, J. Phys.: Condens. Matter **26**, 505301 (2014).
[25] M. Casula, S. Sorella, and G. Senatore, Phys. Rev. B **74**, 245427 (2006).
[26] D. M. Ceperley, Rev. Mod. Phys. **67**, 279 (1995).
[27] I. Kylänpää and T. T. Rantala, J. Chem. Phys. **133**, 044312 (2010).
[28] I. Kylänpää and T. T. Rantala, J. Chem. Phys. **135**, 104310 (2011).
[29] I. Kylänpää, T. T. Rantala, and D. M. Ceperley, Phys. Rev. A **86**, 052506 (2012).
[30] H. J. Schulz, Phys. Rev. Lett. **71**, 1864 (1993).
[31] M. Sassetti and B. Kramer, Phys. Rev. B **54**, R5203 (1996).
[32] M. Sassetti and B. Kramer, Phys. Rev. Lett. **80**, 1485 (1998).
[33] I. Safi and H. J. Schulz, Phys. Rev. B **59**, 3040 (1999).
[34] F. Cavaliere, A. Braggio, J. T. Stockburger, M. Sassetti, and B. Kramer, Phys. Rev. Lett. **93**, 036803 (2004).
[35] K. A. Matveev, Phys. Rev. Lett. **92**, 106801 (2004).
[36] G. A. Fiete, K. Le Hur, and L. Balents, Phys. Rev. B **72**, 125416 (2005); **73**, 165104 (2006); G. A. Fiete, Rev. Mod. Phys. **79**, 801 (2007).
[37] K. A. Matveev, A. Furusaki, and L. I. Glazman, Phys. Rev. Lett. **98**, 096403 (2007).
[38] D. Mantelli, F. Cavaliere, and M. Sassetti, J. Phys.: Condens. Matter **24**, 432202 (2012).
[39] N. Traverso Ziani, F. Cavaliere, and M. Sassetti, Europhys. Lett. **102**, 47006 (2013).
[40] N. Traverso Ziani, F. Cavaliere, and M. Sassetti, New J. Phys. **15**, 063002 (2013).
[41] N. Traverso Ziani, F. Cavaliere, and M. Sassetti, Phys. Rev. B **86**, 125451 (2012).
[42] A. V. Filinov, M. Bonitz, and Yu. E. Lozovik, Phys. Rev. Lett. **86**, 3851 (2001).
[43] J. Böning, A. Filinov, P. Ludwig, H. Baumgartner, M. Bonitz, and Yu. E. Lozovik, Phys. Rev. Lett. **100**, 113401 (2008).
[44] R. P. Feynman, *Statistical Mechanics* (Perseus Books, Reading, MA, 1998).

[45] D. M. Ceperley, J. Stat. Phys. **63**, 1237 (1991).
[46] E. W. Brown, B. K. Clark, J. L. DuBois, and D. M. Ceperley, Phys. Rev. Lett. **110**, 146405 (2013).
[47] N. Metropolis, A. W. Rosenbluth, M. N. Rosenbluth, A. H. Teller, and E. Teller, J. Chem. Phys. **21**, 1087 (1953).
[48] C. Chakravarty, M. C. Gordillo, and D. M. Ceperley, J. Chem. Phys. **109**, 2123 (1998).
[49] R. Egger, W. Häusler, C. H. Mak, and H. Grabert, Phys. Rev. Lett. **82**, 3320 (1999).
[50] B. Reusch and R. Egger, Europhys. Lett. **64**, 84 (2003).
[51] S. Weiss and R. Egger, Phys. Rev. B **72**, 245301 (2005).